

Probing Flavor in semileptonic transitions at High- p_T

L. Allwicher,^a D. A. Faroughy,^b F. Jaffredo,^{c,*} O. Sumensari^d and F. Wilsch^a

^aPhysik-Institut, Universität Zürich,
CH-8057 Zürich, Switzerland

^bDepartment of Physics and Astronomy, Rutgers University, Piscataway, NJ 08854, USA

^cINFN, Pisa Section, 56127 Pisa, Italy

^dIJCLab,

Pôle Théorie (Bat. 210), CNRS/IN2P3 et Université, Paris-Saclay, 91405 Orsay, France

E-mail: lukall@physik.uzh.ch, darius.faroughy@rutgers.edu,

florentin.jaffredo@pi.infn.it, olcyr.sumensari@ijclab.in2p3.fr,

felix.wilsch@physik.uzh.ch

The Drell-Yan processes $pp \rightarrow \ell\nu$ and $pp \rightarrow \ell\ell$ at high transverse momentum can provide important probes of semileptonic transitions that are complementary to low-energy flavor physics observables. We parametrize possible New Physics (NP) contributions to these processes in terms of form-factors, and derive the corresponding bounds by recasting the latest ATLAS and CMS run 2 searches for mono- and di-lepton resonances. Moreover, we study the validity limit of the Standard Model Effective Field Theory (SMEFT) in this regime by comparing the limits obtained for specific tree-level mediators and their EFT equivalent. Both analyses are performed using HighPT, a new Mathematica package for automatic extraction of high- p_T bounds.

41st International Conference on High Energy physics - ICHEP2022
6-13 July, 2022
Bologna, Italy

*Speaker

1. Introduction

Although flavor physics is primarily probed using low-energy observables such as the decay of heavy hadrons, the study of $pp \rightarrow \ell\nu$ and $pp \rightarrow \ell\ell$ at high energies can provide independent and complementary constraints. Previous works on this subject considered either a specific channel or assumed a particular coupling structure [1–6], see also Ref. [7] and references therein. In this work, we combine all the channels probing semileptonic transitions at the LHC for the various leptonic final states: mono-lepton ($e\nu$, $\mu\nu$, $\tau\nu$) and dilepton (ee , $\mu\mu$, $\tau\tau$, $e\mu$, $e\tau$, $\mu\tau$). Using the latest run-II data with 139 fb^{-1} of integrated luminosity in every channel, we are able to constrain all the relevant New Physics (NP) coefficients. We work both in the Standard Model Effective Field Theory (SMEFT) and with various tree-level mediators Beyond the Standard Model (BSM), which can contribute to the non-resonant dilepton production.

Our results are presented in HighPT, a new Mathematica package that provides the complete likelihood for semileptonic operators in Drell-Yan processes at the LHC [8].

2. Form-Factor Parameterization

We start by expressing the partonic scattering amplitude of $\bar{q}_i q_j \rightarrow \ell_\alpha^- \ell_\beta^+$ ($q \in u, d$) and $\bar{u}_i d_j \rightarrow \ell_\alpha^\pm \nu_\beta$ in terms of generic form-factors, where α, β are lepton flavor indices and i, j are quark flavor indices. For the neutral currents, the most generic parameterization consistent with the gauge symmetries reads:

$$\begin{aligned} \mathcal{A}(\bar{q}_i q_j \rightarrow \ell_\alpha^- \ell_\beta^+) = \frac{1}{v^2} \sum_{XY} \left\{ \right. & (\bar{\ell}_\alpha \gamma^\mu \mathbb{P}_X \ell_\beta) (\bar{q}_i \gamma_\mu \mathbb{P}_Y q_j) [\mathcal{F}_V^{XY, qq}(\hat{s}, \hat{t})]_{\alpha\beta ij} \\ & + (\bar{\ell}_\alpha \mathbb{P}_X \ell_\beta) (\bar{q}_i \mathbb{P}_Y q_j) [\mathcal{F}_S^{XY, qq}(\hat{s}, \hat{t})]_{\alpha\beta ij} \\ & + (\bar{\ell}_\alpha \sigma_{\mu\nu} \mathbb{P}_X \ell_\beta) (\bar{q}_i \sigma^{\mu\nu} \mathbb{P}_Y q_j) \delta^{XY} [\mathcal{F}_T^{XY, qq}(\hat{s}, \hat{t})]_{\alpha\beta ij} \quad (1) \\ & + (\bar{\ell}_\alpha \gamma_\mu \mathbb{P}_X \ell_\beta) (\bar{q}_i \sigma^{\mu\nu} \mathbb{P}_Y q_j) \frac{ik_\nu}{v} [\mathcal{F}_{D_q}^{XY, qq}(\hat{s}, \hat{t})]_{\alpha\beta ij} \\ & \left. + (\bar{\ell}_\alpha \sigma^{\mu\nu} \mathbb{P}_X \ell_\beta) (\bar{q}_i \gamma_\mu \mathbb{P}_Y q_j) \frac{ik_\nu}{v} [\mathcal{F}_{D_\ell}^{XY, qq}(\hat{s}, \hat{t})]_{\alpha\beta ij} \right\}, \end{aligned}$$

where $X, Y \in \{L, R\}$ are the chiralities of the anti-lepton and anti-quark fields, $\mathbb{P}_{R,L} = (1 \pm \gamma^5)/2$ are the chirality projectors, $v = (\sqrt{2}G_F)^{-1/2}$ stands for the electroweak vacuum-expectation-value (vev), and fermion masses have been neglected. $k = p_q + p_{\bar{q}}$, and we take the Mandelstam variables to be $\hat{s} = k^2 = (p_q + p_{\bar{q}})^2$, $\hat{t} = (p_q - p_{\ell^-})^2$ and $\hat{u} = (p_q - p_{\ell^+})^2 = -\hat{s} - \hat{t}$. We perform a similar expansion for the charged processes [7].

Each process can thus be written in terms of the $[\mathcal{F}_I^{XY, qq}(\hat{s}, \hat{t})]_{\alpha\beta ij}$, depending on 4 flavor indices, 2 chiralities, for 5 Lorentz structures: vector, scalar, tensor, lepton dipole, and quark dipole. The form-factors are dimensionless functions of the Mandelstam variables s , t , and $u = -s - t$. Furthermore, we assume that form-factors can be expressed as the sum of an analytic function and a finite number of simple poles:

$$\mathcal{F}_I(\hat{s}, \hat{t}) = \mathcal{F}_{I, \text{Reg}}(\hat{s}, \hat{t}) + \mathcal{F}_{I, \text{Poles}}(\hat{s}, \hat{t}). \quad (2)$$

By doing so, we encapsulate every possible tree-level dynamic. The regular part can be expanded to express all the possible contact interactions and be matched to the SMEFT Lagrangian. Instead, the pole terms encode the SM tree-level interactions (Photon, Z, and W poles) and their effective modifications, as well as any tree-level NP mediator in the s , t , and u channels. The matching of the form-factors to the SMEFT and BSM mediators can be found in Ref. [7].

Using these form-factors, the partonic cross-section can be computed as

$$\frac{d\hat{\sigma}}{d\hat{t}}(\bar{q}_i q'_j \rightarrow \ell_\alpha \bar{\ell}'_\beta) = \frac{1}{48\pi v^4} \sum_{XY} \sum_{IJ} M_{IJ}^{XY}(\hat{s}, \hat{t}) \left[\mathcal{F}_I^{XY, qq'}(\hat{s}, \hat{t}) \right]_{\alpha\beta ij} \left[\mathcal{F}_J^{XY, qq'}(\hat{s}, \hat{t}) \right]_{\alpha\beta ij}^*, \quad (3)$$

where M_{IJ}^{XY} are matrices describing the interference between the various form-factors. This partonic cross-section must be convoluted with the parton-parton luminosity functions and integrated over the detector phase space. See Ref. [7] for details. Schematically, for the SMEFT expansion at order $1/\Lambda^4$ the cross-section takes the following shape:

$$\hat{\sigma} \sim \int [d\Phi] \left\{ |\mathcal{A}_{\text{SM}}|^2 + \frac{v^2}{\Lambda^2} \sum_i 2 \text{Re}(\mathcal{A}_i^{(6)} \mathcal{A}_{\text{SM}}^*) + \frac{v^4}{\Lambda^4} \left[\sum_{ij} 2 \text{Re}(\mathcal{A}_i^{(6)} \mathcal{A}_j^{(6)*}) + \sum_i 2 \text{Re}(\mathcal{A}_i^{(8)} \mathcal{A}_{\text{SM}}^*) \right] + \dots \right\}, \quad (4)$$

where $[d\Phi]$ denotes the corresponding Lorentz invariant phase-space measure, \mathcal{A}_{SM} is the SM amplitude, and $\mathcal{A}_i^{(6)}$ and $\mathcal{A}_i^{(8)}$ stand for the New Physics contributions from dimension-6 and dimension-8 operators, respectively. The interference between the dimension-8 and the SM appears at the same order as the dimension-6 squared term.

The classes of SMEFT operators contributing to the cross section are listed in Tab. 1 with their energy scaling. Some of them exhibit an energy enhancement compared to the SM amplitude, making it possible to extract bounds by looking at the tail of the p_T distributions in colliders.

Dimension		$d = 6$			$d = 8$			
		ψ^4	$\psi^2 H^2 D$	$\psi^2 XH$	$\psi^4 D^2$	$\psi^4 H^2$	$\psi^2 H^4 D$	$\psi^2 H^2 D^3$
Operator classes		ψ^4	$\psi^2 H^2 D$	$\psi^2 XH$	$\psi^4 D^2$	$\psi^4 H^2$	$\psi^2 H^4 D$	$\psi^2 H^2 D^3$
Amplitude scaling		E^2/Λ^2	v^2/Λ^2	vE/Λ^2	E^4/Λ^4	$v^2 E^2/\Lambda^4$	v^4/Λ^4	$v^2 E^2/\Lambda^4$
Parameters	# Re	456	45	48	168	171	44	52
	# Im	399	25	48	54	63	12	12

Table 1: Counting of SMEFT parameters relevant to the high- p_T observables and the corresponding energy scaling of the amplitude for each class of operators. The number of real and imaginary free parameters that contribute to the Drell-Yan cross-sections at order $\mathcal{O}(1/\Lambda^4)$ are listed for each operator class.

3. Collider limits

In order to compare our theoretical prediction for the cross-section with the events reported by ATLAS and CMS for mono-lepton ($e\nu$, $\mu\nu$, $\tau\nu$) and dilepton channels (ee , $\mu\mu$, $\tau\tau$, $e\mu$, $e\tau$, $\mu\tau$), we need to take into account the imperfections of the detector. The differential distributions are measured with a finite energy resolution over a limited acceptance. The final states are sometimes observed through their decays (e.g. hadronic tau) or from the missing transverse energy (neutrinos).

We encode the difference between a predicted distribution over a particle-level observable x and the detector-level observable x_{obs} through the convolution

$$\frac{d\sigma}{dx_{\text{obs}}} = \int dx K(x_{\text{obs}}|x) \frac{d\sigma}{dx}, \quad (5)$$

where $K(x_{\text{obs}}|x)$ is a kernel function that parametrizes the detector response. After binning over x and x_{obs} , K becomes an efficiency matrix, with K_{AB} the probability for an event in bin B of x to pass the various triggers and selection cuts and end up in bin A of x_{obs} . This probability depends heavily on the kinematic of the event, which is different for the various combinations of form-factors. From Eq. (2,3) we see that the cross-section can be expressed as a sum of interfering form-factors, each multiplied by a single scalar coefficient. It is thus sufficient to estimate this probability for every term independently and sum the resulting visible cross-sections.

We use Monte Carlo simulations to estimate the efficiency matrix. For every combination of interfering form-factors, we generate 50000 events per bin using MadGraph5 [9]. The events are then showered and hadronized using Pythia8 [10]. The simulation of the detector and the reconstruction of the events is then performed by Delphes3 [11], reproducing the cuts and selections of the specific ATLAS and CMS searches, see e.g. [12, 13] and Refs. within [7]. Details for each search are given in Ref. [7].

To compare the observed number of events with our predictions, we build a Pearson's χ^2 test statistic using the background and background uncertainty provided by the experimental collaborations and assuming a Poissonian error in the signal:

$$\chi^2(\theta) = \sum_{A \in \mathcal{A}} \frac{(\mathcal{N}_A(\theta) + \mathcal{N}_A^b - \mathcal{N}_A^{\text{obs}})^2}{(\delta \mathcal{N}_A^b)^2 + \mathcal{N}_A^{\text{obs}}}, \quad (6)$$

We observe no significant excess of events, but we are able to constrain all the coefficients collected in Tab. 1. The full χ^2 defined as a polynomial in the NP coefficients is made available in the package HighPT [8]. See Fig. 1 for a result example.

4. Validity of the EFT expansion

Using HighPT, we are able to test various claims concerning the validity of the EFT expansion for the high- p_T tails observables.

- **SMEFT truncation, $\mathcal{O}(1/\Lambda^2)$ or $\mathcal{O}(1/\Lambda^4)$:**

At order $\mathcal{O}(1/\Lambda^2)$, only the dimension-6 operators interfering with the SM contribute. Even for those operators, we found the $\mathcal{O}(1/\Lambda^4)$ terms to give significant contributions thanks to their energy enhancements.

- **EFT or explicit mediator:**

If the scale of NP is expected to be around a few TeV, the EFT approximation could introduce sizable errors in our computation, especially in the high- p_T region, which is crucial for the extraction of our bounds, due to the energy enhancement of the cross-section. Even for non-resonant processes, we found $\mathcal{O}(1)$ effects for masses below 2 TeV. To ensure the validity of the EFT approximation, one can introduce a clipping in the analysis to enforce the separation of scale between the EFT scale and the energy of the events. This results in a mild weakening of the bounds. The effects of the energy clipping, as well as the order of the EFT truncation, are illustrated in Fig. 1.

- **Impact of dimension 8 operators:**

While contributing at $\mathcal{O}(1/\Lambda^4)$, the dimension-8 operators have been found to be relevant in a limited mass range only for first generation quarks, and only if the dimension-6 and dimension-8 couplings are uncorrelated, which usually does not happen when matching to explicit scenarios.

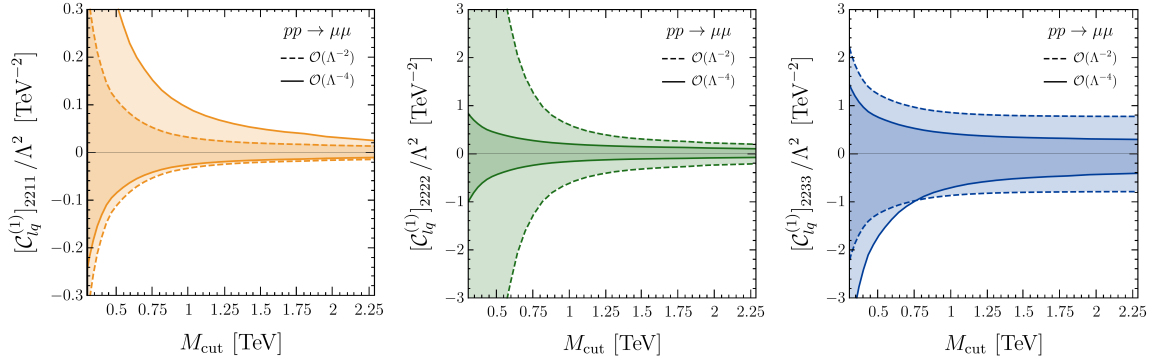


Figure 1: Clipped expected limits from LHC dimuon searches for flavor conserving operators $\mathcal{O}_{lq}^{(1)}$ as a function of the sliding maximal scale M_{cut} . The dashed and solid contours correspond to the EFT truncation at $\mathcal{O}(1/\Lambda^2)$ and $\mathcal{O}(1/\Lambda^4)$, respectively.

5. Summary and perspectives

We provided for the first time the complete high- p_T Drell-Yan likelihood for the full set of energy-enhanced $d \leq 8$ SMEFT operators, with arbitrary flavor indices. This was achieved by recasting the most recent run-II data sets by ATLAS and CMS in the mono-lepton ($e\nu$, $\mu\nu$, $\tau\nu$) and dilepton channels (ee , $\mu\mu$, $\tau\tau$, $e\mu$, $e\tau$, $\mu\tau$). Our results are presented in a package `HighPT` [8], which also supports some tree-level mediators scenarios, allowing us to explicitly check the validity of the EFT approximation.

This study leaves room for many improvements: (i) the inclusion of additional experimental searches increasing the sensitivity, (ii) the joint determination of PDF and BSM couplings for better control of the uncertainties, (iii) the implementation of double-differential distributions, as well as (iv) a model-independent combination of our high-energy limits with electroweak and low-energy flavor data.

References

- [1] D. A. Faroughy, A. Greljo and J. F. Kamenik, Phys. Lett. B **764** (2017), 126-134 doi:10.1016/j.physletb.2016.11.011 [arXiv:1609.07138 [hep-ph]].
- [2] A. Greljo and D. Marzocca, Eur. Phys. J. C **77** (2017) no.8, 548 doi:10.1140/epjc/s10052-017-5119-8 [arXiv:1704.09015 [hep-ph]].
- [3] A. Greljo, J. Martin Camalich and J. D. Ruiz-Álvarez, Phys. Rev. Lett. **122** (2019) no.13, 131803 doi:10.1103/PhysRevLett.122.131803 [arXiv:1811.07920 [hep-ph]].
- [4] M. Endo, S. Iguro, T. Kitahara, M. Takeuchi and R. Watanabe, JHEP **02** (2022), 106 doi:10.1007/JHEP02(2022)106 [arXiv:2111.04748 [hep-ph]].
- [5] S. Iguro, M. Takeuchi and R. Watanabe, Eur. Phys. J. C **81** (2021) no.5, 406 doi:10.1140/epjc/s10052-021-09125-5 [arXiv:2011.02486 [hep-ph]].
- [6] A. Angelescu, D. A. Faroughy and O. Sumensari, Eur. Phys. J. C **80** (2020) no.7, 641 doi:10.1140/epjc/s10052-020-8210-5 [arXiv:2002.05684 [hep-ph]].
- [7] L. Allwicher, D. A. Faroughy, F. Jaffredo, O. Sumensari and F. Wilsch, [arXiv:2207.10714 [hep-ph]].
- [8] L. Allwicher, D. A. Faroughy, F. Jaffredo, O. Sumensari and F. Wilsch, [arXiv:2207.10756 [hep-ph]].
- [9] J. Alwall, R. Frederix, S. Frixione, V. Hirschi, F. Maltoni, O. Mattelaer, H. S. Shao, T. Stelzer, P. Torrielli and M. Zaro, JHEP **07** (2014), 079 doi:10.1007/JHEP07(2014)079 [arXiv:1405.0301 [hep-ph]].
- [10] T. Sjöstrand, S. Ask, J. R. Christiansen, R. Corke, N. Desai, P. Ilten, S. Mrenna, S. Prestel, C. O. Rasmussen and P. Z. Skands, Comput. Phys. Commun. **191** (2015), 159-177 doi:10.1016/j.cpc.2015.01.024 [arXiv:1410.3012 [hep-ph]].
- [11] J. de Favereau *et al.* [DELPHES 3], JHEP **02** (2014), 057 doi:10.1007/JHEP02(2014)057 [arXiv:1307.6346 [hep-ex]].
- [12] G. Aad *et al.* [ATLAS], Phys. Rev. Lett. **125** (2020) no.5, 051801 doi:10.1103/PhysRevLett.125.051801 [arXiv:2002.12223 [hep-ex]].
- [13] A. M. Sirunyan *et al.* [CMS], JHEP **07** (2021), 208 doi:10.1007/JHEP07(2021)208 [arXiv:2103.02708 [hep-ex]].